Using IR Brightness Temperature Spectra to Disentangle the Effects of Ozone, Carbon Dioxide, and Water Vapor On Global Stratospheric Temperature Trends

Ester Nikolla, Robert Knuteson, Michelle Feltz, and Henry Revercomb

University of Wisconsin-Madison Space Science and Engineering Center (SSEC)
Cooperative Institute for Meteorological Satellite Studies (CIMSS)

1. INTRODUCTION

Global carbon dioxide (CO_2) concentrations have been steadily increasing for the last 50 years. The increase in global CO_2 concentration has been predicted to cause a cooling effect in the stratosphere due to increased infrared radiative emission to space from the 15 μm absorption band of CO_2 (Ramaswamy et al. 2001).

Ozone (O_3) is a triatomic molecule and a powerful oxidizing agent. The formation of ozone in the stratosphere is initiated by ultraviolet (UV) sunlight and results in the reaction of molecular oxygen (O_2) and atomic oxygen (O) in the presence of a third body, e.g. nitrogen. It absorbs energy from the reaction as heat. Without this absorption, the combining of O and O_2 into ozone cannot be completed.

The Montreal Protocol on Substances that Deplete the Ozone Layer enacted in 1987, banned the production of CFCs. The stratospheric ozone levels are expected to recover over the next 50 years. This increase in ozone concentration is expected to contribute a warming effect in the stratosphere, which is expected to compensate for the cooling effect of increasing carbon dioxide concentrations in the stratosphere (Seidel et al. 2016; Maycock 2016).

The detection of temperature trends in the stratosphere has proven challenging due to lack of well-calibrated measurements from in situ (weather balloon borne radiosondes) and satellite passive IR and microwave sensors. (Randel et al. 2009). The recent record of radio occultation (RO) measurements from space provides a new set of global temperature observations but with significant sampling only since 2007 (Steiner et al. 2013, 2011; Ho et al. 2010). Another recent development is the use of accurate spectrally resolved infrared radiance to investigate trends in infrared brightness temperature (Huang and Ramaswamy 2009, Tobin et al. 2013, Pan et al. 2015). Initial comparisons between RO and IR observations indicate that the lower stratosphere is a region where both measurements have shown good agreement of approximately a few tenths of a degree Celsius (Feltz et al. 2014). The use of SI traceable measurements from space in the measurement of climate temperature trends is the goal of the CLARREO mission (Wielicki et al. 2013). The time to detect trends is a combination of the natural variability and measurement error plus any autocorrelation of the time series.

The objective of this study is to investigate the correlation of the infrared brightness temperature spectra from Earth orbiting satellites with time and space coincident vertical profiles of atmospheric ozone concentration and atmospheric temperature. Vertical profiles are computed in ten-degree latitude zones along with corresponding infrared brightness temperature mean spectra.

2. DATA

The data used in this study are from the Cross-track InfraRed Sounder (CrIS) and the Ozone Mapping Profiler Suite (OMPS) on the NASA Suomi-NPP satellite platform. Figure 1 shows the CrIS and OMPS on the nadir viewing deck of the Suomi-NPP satellite. The Suomi-NPP satellite is in a sun-synchronous polar orbit with a 1:30 pm equator crossing time, similar to the NASA Aqua satellite but at a higher altitude. The Suomi-NPP satellite has an instrument suite which closely matches that of the operational Joint Polar Satellite System (JPSS) expected to be launched in early 2017.

The Cross-track Infrared Sounder (CrIS), provides soundings of the atmosphere with 1305 spectral channels, over 3 wavelength ranges: LW (9.14 - 15.38um); MW (5.71 - 8.26um); and SW (3.92 - 4.64 um). The longwave band resolution is 0.625 cm^{-1}. The CrIS instrument is a Fourier transform spectrometer which records the interference pattern of the infrared wavelengths which are contained in each of the LW, MW, and SW spectral bands. As the satellite orbits from pole to pole, the CrIS sensor uses a 45 degree mirror to scan a 2200km swath width (+/- 50 degrees), with 30 Earth-scene fields of regard. Each field of regard consists of 9 fields of view, arrayed as 3x3 array of 14km diameter spots (at nadir). This yields 90 Earth views across track. Each scanline includes views of the internal calibration target (warm calibration point), and a deep space view (cold calibration point). The

CrIS sensor on Suomi-NPP has demonstrated excellent absolute accuracy (Tobin et al. 2013).

Figure 1. Photo image of the NASA Suomi-NPP satellite with labels for the five sensors. (https://jointmission.gsfc.nasa.gov/cris.html)

The raw CrIS interferogram packets used in this study were obtained from the NOAA CLASS archive (http://www.class.ncdc.noaa.gov). In order to create a consistent radiance record, the CrIS radiance spectra were reprocessed at the University of Wisconsin-Madison Space Science and Engineering Center (SSEC) using JPSS software available for use with direct broadcast. (http://cimss.ssec.wisc.edu/cspp/npp_sdr_v2.2.3.shtml).

Vertical profiles of ozone concentration along the nadir satellite track of Suomi-NPP were obtained from the NASA OMPS science team archive at https://ozoneaq.gsfc.nasa.gov/data/omps/. An example OMPS Limb Profiler daily product data file is name OMPS-NPP_LP-L2-O3-DAILY_v2.3_....h5. The spectral measurements from the OMPS of the solar radiances scattered by the Earth's atmosphere are used to generate estimates of the ozone vertical profile along the orbital track. For the combined ozone density profile used here, the VIS retrieval results are used between 0-26.5 km, and the UV retrieval results are used between 27.5-60.5 km. The temperature profiles used in this study were extracted from the OMPS Limb Profiler daily product file from the NASA GMAO GEOS-5. (http://ozoneaq.gsfc.nasa.gov/omps/media/docs/LP-L2-O3-DAILY_V2_Product_Description.pdf)

3. METHODOLOGY

The CrIS radiance spectra near nadir were extracted from the CrIS cross-track scanlines for each UTC day. The two CrIS fields of view that bracket the satellite nadir track (element 45 and 46 out of 90) were selected. A daily nadir CrIS radiance file was created that contained all three CrIS spectral bands for each day from 1 April 2012 through 31 March 2016. A set of zonal mean radiance spectra were computed for each day of the three-year period using 10-degree latitude bins. The CrIS zonal brightness temperature spectra used in this study contain the average of both sunlit and nighttime portions of the latitude zone. The zonal mean radiances were converted to brightness temperature spectra using a Planck curve at the scene radiance to find the equivalent blackbody temperature. A global mean radiance was computed by weighting each latitude zone average radiance spectrum by the cosine of the mean latitude. This is equivalent to an area weighted average. The corresponding global mean brightness temperature was computed from the global mean radiance spectrum for each day.

Two CrIS brightness temperature (BT) spectral channels were selected which peak in the upper stratosphere (667.5 cm^{-1}) and the lower stratosphere (680.0 cm^{-1}). The channel width of each is 0.625 cm^{-1}. The vertical sensitivity functions of these two channels was computed using the Optimal Spectral Sampling (OSS) method of AER, Inc. for the standard AFGL atmospheric climatology. These sensitivity functions are shown in Figure 2 and indicate that the variation by latitude zone is fairly small.

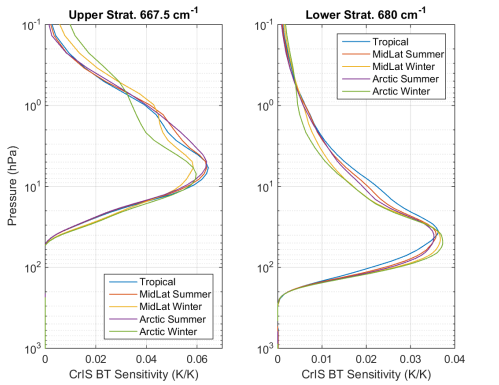

Figure 2. CrIS vertical sensitivity functions for the upper stratosphere (left) and lower stratosphere (right). The colored lines indicate variations in the indicated channel sensitivity due to climatological latitude zone and season.

The daily zonal mean OMPS ozone density profiles were computed using a method very similar to that used in creating the daily mean zonal CrIS brightness temperatures. The OMPS has three near nadir profiles for each scan line. All three profiles were included in the calculation of 10-degree zone mean profiles for each day of the year from April 2012 through March 2016. Since OMPS relies on sunlight as a source, there are no OMPS ozone profiles on the dark side of the Earth.

The CrIS vertical sensitivity functions were used to weight the OMPS ozone density profiles to create a comparison in the upper and lower stratosphere which best represents the CrIS spectral channels. The vertical weights shown in Figure 6 were used based upon the latitude zone which best matched the AFGL climatology. A similar method was used to vertically weight the atmospheric temperature profiles.

4. RESULTS

Figure 3 illustrates the time series of the OMPS data for each day between April 2012 and March 2016 for selected latitude zones. For these same zones the CrIS sensitivity functions were used to compute a weighted average OMPS ozone layer corresponding to the CrIS vertical sensitivity shown in Figure 2. The equatorial zone shows relatively constant CrIS brightness temperatures and constant weighted mean OMPS ozone amounts. CrIS BT seasonal variations are apparent in mid-latitudes and largest in the 65N and 65S latitude zones. In the upper stratosphere, the CrIS and OMPS seasonal variations are in phase, however, the CrIS BT seems to lag the OMPS ozone by about six months in the lower stratosphere.

Scatterplots of the time series of daily CrIS and OMPS data are shown in Figure 3. In the upper stratosphere there is a larger correlation of CrIS BT with OMPS ozone amount in the extra-tropics. In the lower stratosphere only the 65S zone shows significant correlation between CrIS and OMPS. Short time scale deviations in both BT and Ozone reduce the correlation by increasing scatter.

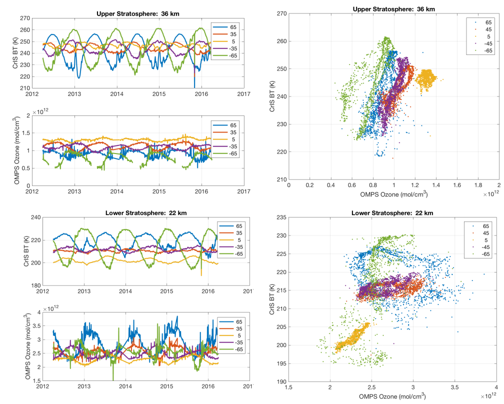

Figure 3. Zonal Mean CrIS BT and OMPS Ozone time series and scatterplot.

Figure 4 illustrates the time series of the GEOS-5 atmospheric temperature for the layers corresponding to the CrIS brightness temperatures. Very high correlation is seen between CrIS BT and layer temperature for the upper stratosphere channel. Poorer correlation is seen in the lower stratosphere.

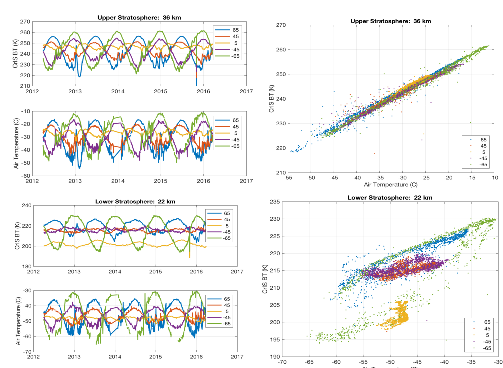

Figure 4. Zonal Mean CrIS BT and Atmospheric Temperature time series and scatterplot.

Figure 5 depicts the combined ozone value over a time series of ~4 years, as well as the atmospheric temperature over the same time period. In the summer months, when the temperature is hotter, the tropopause altitude (black line) increases in height noticeably in the mid latitude zones due to the hot air rising. There is no variability in the tropopause altitude in the tropical zones due to the fact that the sun is shining on that area year round. There is also little to no variability at -55 degrees due to the fact that there are no large land masses present in that area. As the tropopause altitude increases, it is observed that the ozone concentration in the lower stratosphere decreases. This is seen predominantly in the mid latitude zones during the summer months.

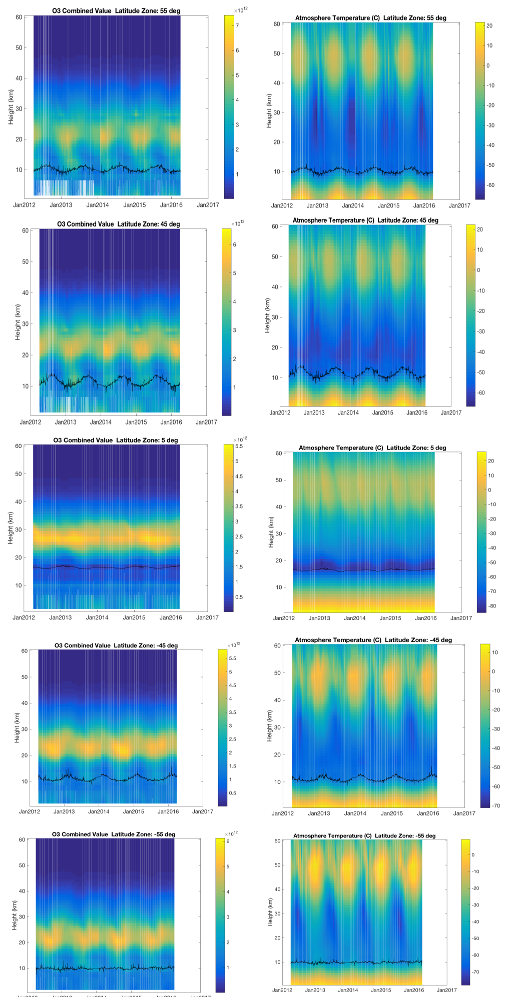

Figure 5. Ozone (left) and Atmospheric temperature (right) time height cross sections for April 2012 to March 2016.

5. CONCLUSION

A preliminary investigation of the correlation of CrIS infrared brightness temperature variations in the upper and lower stratosphere with OMPS ozone profiles from the same satellite platform has been performed. This study compared CrIS zonal mean brightness temperatures to OMPS zonal mean ozone profiles weighted by the CrIS vertical sensitivity. Seasonal and zonal variations of the CrIS and OMPS observations are most apparent outside the topical zone. In general, the upper stratosphere has higher correlation between infrared brightness temperatures and ozone amount than the lower stratosphere. The exception is the 65S zone of the lower stratosphere where the correlation is comparable. A lag of about six months between infrared brightness temperature and ozone amount is seen in the northern hemisphere lower stratosphere. The complex relationship of IR brightness temperatures and ozone amounts requires further investigation.

Analysis of coincident CrIS BT and atmospheric temperature shows a high correlation for the upper stratosphere. A poorer correlation is seen in the lower stratosphere.

Additional investigation is required to obtain a complete understanding of the role of ozone and carbon dioxide in regards to future trends in stratospheric temperature. NOAA Carbon Tracker will be used to determine the correlation of CrIS BT with carbon dioxide amount. We can then utilize the ozone, temperature, and carbon dioxide observations explain the variance in the CrIS BT zonal interannual variability.

Acknowledgments

The authors acknowledge the support of NASA ROSES grant NNX15AC26G and correspondence with H. Brindley and R. Bantges of Imperial College.

References

Brindley, H., Bantges, R., Russell, J., Murray, J., Dancel, C., Belotti, C. and Harries, J. (2015), Spectral signatures of Earth's climate variability over 5 years from IASI. *Journal of Climate*, *28*(4), pp.1649-1660.

Feltz, M. L., Knuteson, R. O., Revercomb, H. E., & Tobin, D. C. (2014), A methodology for the validation of temperature profiles from hyperspectral infrared sounders using GPS radio occultation: Experience with AIRS and COSMIC. Journal of Geophysical Research: Atmospheres, 119(3), 1680-1691.

Ho, S.-P., Y.-H. Kuo, W. Schreiner, and X. Zhou (2010), Using SI-traceable Global Positioning System radio occultation measurements for climate monitoring, Bull. Am. Meteorol. Soc., 91(7), S36–S37.

Huang, Y. and V. Ramaswamy (2009), Evolution and trend of the outgoing longwave radiation

spectrum. J. Climate, 22, 4637-4651, doi:10.1175/2009JCLI2874.1.
Kramarova, N. A., Nash, E. R., Newman, P. A., Bhartia, P. K., McPeters, R. D., Rault, D. F., ... & Labow, G. J. (2014). Measuring the Antarctic ozone hole with the new Ozone Mapping and Profiler Suite (OMPS). *Atmospheric Chemistry and Physics*, *14*(5), 2353-2361

Maycock, A. C., 2016: The contribution of ozone to future stratospheric temperature trends, Geophysical Research Letters, doi: 10.1002/2016GL068511

Pan, F., X. Huang, L. Strow, and H. Guo, 2015: Linear trends and closures of 10-year observations of AIRS stratospheric channels. J. Climate. doi:10.1175/JCLID-15-0418.1

Ramaswamy, et al., 2001: Stratospheric temperature trends: Observations and model simulations. Rev. Geophys., 39, 71-122.

Randel, W. J., et al. (2009), An update of observed stratospheric temperature trends, J. Geophys. Res., 114, D02107, doi:10.1029/2008JD010421.

Seidel, D. J.,et al., 2016: Stratospheric temperature changes during the satellite era, J. Geophys. Res. Atmos., 121, 664–681, doi:10.1002/2015JD024039.

Steiner, A. K., et al. (2011), GPS radio occultation for climate monitoring and change detection, Radio Sci., 46, RS0D24, doi:10.1029/2010RS004614.

Steiner, A. K., Hunt, D., Ho, S. P., Kirchengast, G., Mannucci, A. J., Scherllin-Pirscher, B., ... & Leroy, S. S. (2013). Quantification of structural uncertainty in climate data records from GPS radio occultation. Atmospheric Chemistry and Physics, 13(3), 1469-1484.

Tobin, David, et al. (2013), Suomi-NPP CrIS radiometric calibration uncertainty. Journal of Geophysical Research: Atmospheres 118.18.

Wielicki, B., et al., 2013: Achieving Climate Change Absolute Accuracy in Orbit. BAMS., 94, 1519+.